Supporting Information

Luminescence Enhancement through Co-sensitization in Lanthanide Composites for Efficient Photocatalysis

Langtao Ren,[a] Qing Zhao,[a] Yan Su,[b] Mingzhu Zhou,[a,c]* and Qianqian Su[a]*

[a]Institute of Nanochemistry and Nanobiology, Shanghai University, Shanghai 200444, China.
[b]Genome Institute of Singapore, Agency of Science Technology and Research, 138672, Singapore.
[c]College of Geography and Environmental Sciences, Zhejiang Normal University, Jinhua 321004, China

*Corresponding authors: Q. Su, Email: chmsqq@shu.edu.cn; M.Zhou, Email: mzzhou@zjnu.edu.cn

1. Experimental Section

1.1 Materials: $Gd(CH_3CO_2)_3{\cdot}xH_2O$ (99.9%), $Y(CH_3CO_2)_3{\cdot}xH_2O$ (99.9%), $Yb(CH_3CO_2)_3{\cdot}xH_2O$ (99.9%), $Tm(CH_3CO_2)_3{\cdot}xH_2O$ (99.9%), $Er(CH_3CO_2)_3{\cdot}xH_2O$ (99.9%), $Tb(CH_3CO_2)_3{\cdot}xH_2O$ (99.9%), $Eu(CH_3CO_2)_3{\cdot}xH_2O$ (99.9%), $Ce(CH_3CO_2)_3{\cdot}xH_2O$ (99.9%), $Dy(CH_3CO_2)_3{\cdot}xH_2O$ (99.9%), $Sm(CH_3CO_2)_3{\cdot}xH_2O$ (99.9%), NaOH (>98%), NH_4F (>98%), oleic acid (OA, 90%), 1-octadecene (ODE, 90%), TiF_4 were all purchased from Sigma-Aldrich. L-cysteine, Cadmium nitrate, polyvinylpyrrolidone (PVP, Mw = 40,000), Cyclohexane (AR) and ethanol (AR) were purchased from Aladdin. All chemicals were used as received without further purification.

1.2 Synthesis of $NaYbF_4$ core nanoparticles.

$NaYbF_4$ nanoparticles were synthesized according to a modified literature procedure[1]. $Yb(CH_3CO_2)_3$ (4 ml, 0.8 mmol), ODE (10 mL), and OA (10 mL) were added into a three-neck reaction flask and heated at 150 °C for 1.5 h to form the lanthanide-oleate precursor. After cooling to room temperature naturally, sodium oleate (6.4 mmol) was added to the mixture and stirred for 1 h at 100 °C under vacuum conditions. NH_4F (3.2 mmol) was then added to the reaction mixture under abundant nitrogen atmosphere, and the mixture was slowly raised to 160 °C and kept this temperature for 1.5 h. Afterward, the reaction mixture was evaporated at this temperature for 10 min under vacuum before the reaction temperature was heated to 320 °C with a constant heating rate and kept for 30 min under nitrogen. Subsequently, the reaction was cooled down to room temperature, the obtained nanoparticles were precipitated using ethanol by centrifugation at 8000 rpm for 5 min, and washed with ethanol and cyclohexane for three times. The purified core nanoparticles were re-dispersed in 8 mL of cyclohexane for further shell coating. The synthesis procedures of other core nanoparticles were the same as the synthesis procedures of $NaYbF_4$ core nanoparticles, except that the precursor solution of the core with different dopant composition was used.

1.3 Synthesis of $NaYbF_4$@$NaGdF_4$:49%Yb,1%Tm core-shell nanoparticles.

The synthesis process of core-shell nanoparticles was similar to that reported in our previous report[2]. The pre-synthesized $NaYbF_4$ core nanoparticles were used as seeds for shell coating. In a typical experiment, the aqueous solution of $Gd(CH_3CO_2)_3$ (0.2 mmol), $Yb(CH_3CO_2)_3$ (0.2 mmol), and $Tm(CH_3CO_2)_3$ (0.004 mmol) were added to a mixture of OA (5 mL), and ODE (5 mL) in a two-necked flask at room temperature. The mixture was stirred at 150 °C for 1 hour. After cooling down to 80 °C, 4 mL cyclohexane solution of $NaYbF_4$ core nanoparticles were added to the reaction system and kept for 30 min to remove cyclohexane. Thereafter, a methanol solution of NH_4F (3.4 mL, 0.4 M) and NaOH (1 mL, 1 M) was added and stirred at 50 °C for 30 min. The reaction then maintained at 100 °C for 20 min to remove impurities, and heated at 300 °C for 1.5 h under a nitrogen atmosphere. After the reaction mixture was cooled down to room temperature, the obtained core-shell nanoparticles were collected by the addition of ethanol and washed for three times before dispersion in cyclohexane.

1.4 Synthesis of $NaYbF_4$@$NaGdF_4$:49%Yb,1%Tm@$NaYF_4$:10%Yb core-multishell nanoparticles.

The synthesis process of core-multishell nanoparticles is the same as that of core-shell nanoparticles, except that $NaYF_4$ shell solution with or without the Yb dopant is used. In addition, the synthetic procedure for core-multishell nanoparticles using $NaYF_4$ as the host matrix was identical to that for $NaGdF_4$ core-multishell nanoparticles except for the use of a stock solution of Y^{3+} and OA (3 mL) and ODE (7 mL) and a final reaction temperature of 290°. The preparation process of other core-multishell nanoparticles were similar to that for core-shell nanocrystals apart from the use of a shell stock solution with different lanthanide dopants.

1.5 Synthesis of ligand-free nanoparticles.

Ligand-free nanoparticles were prepared based on a reported literature procedure[3]. A total of 1 mL of a cyclohexane solution of the OA-capped core- multishell nanoparticles (0.1 mmol) was precipitated by adding 1.5 mL of ethanol. The solid was obtained by centrifugation and redispersed in 2.0 mL of ethanol. After adding of 1.0-mL HCl (0.2 M), the slurry was sonicated at room temperature for 10 min to remove the OA ligands. The ligand-free nanoparticles were collected by centrifugation at 12000 rpm for 15 min, washed with ethanol for twice times, and then redispersed in deionized water (1 mL).

1.6 Synthesis of Yb@Tm@Yb@TiO_2 hybrid nanocomposites.

Yb@Tm@Yb@TiO_2 nanocomposites were synthesized according to a modified literature procedure[4]. In a typical synthesis procedure, 1 mL of prepared ligand-free nanoparticles were added into 4 mL of aqueous solution containing 1.0 g polyvinylpyrrolidone with the aid of stirring and ultrasonication. After addition of ethanol (20 mL), the mixture was stirred at room temperature for 30 min, then TiF_4 aqueous solution (4 mL, 25 mM) was dropwise added into the reacation mixture under vigorous stirring. The final mixture was transferred into a 50 mL Teflon-lines autoclave and heated at 180 °C for 6 h, followed by cooling to the room temperature

naturally. The as-prepared products were isolated by centrifugation (8000 rpm, 10 min) and washed with deionized water and ethanol (the volume ratio of 1:1) several times, and dried at 60 °C.

1.7 Synthesis of Yb@Tm@Yb@TiO_2@CdS hybrid nanocomposites.

Yb@Tm@Yb@TiO_2@CdS nanocomposites were synthesized according to a modified literature procedure[5]. The l-cysteine (0.1 mmol) and cadmium nitrate (0.05 mmol) were mixed in 2 mL deionized water under vigorous stirring at room temperature for 30 min. Thereafter, Yb@Tm@Yb@TiO_2 nanoparticles was dropwise added into the mixture, followed by stirring for another 1 h to form the coupling between cysteine and Yb@Tm@Yb@TiO_2. The reacation mixture was then diluted to 40 mL with deionized water and transferred to a 50 mL Teflon-lined autoclave and heated at 130 °C for 6 h. After cooling down to room temperature naturally, the products was obtained by centrifugation (6000 rpm, 15 min) and washed with deionized water and ethanol (the volume ratio of 1:1) several times. The final solid powder was obtained by drying at 60 °C.

1.8 Photocatalytic activity measurements.

Tetracycline was utilized as a model contaminant to evaluate the photocatalytic activity of the NPs. In a representative measurement, 10 mg of photocatalyst was added to 50 mL of tetracycline solution (10 mg/L). The suspension was constantly stirred in the dark for 1 h to establish the adsorption−desorption equilibrium. Thereafter, a 300 W xenon lamp with a UV-Vis cutoff filter (>700 nm) was employed for irradiation during the experiment. After that, 3 mL of sample was taken out from the reaction system every 30 min, and the photocatalyst in the sample was filtered through a 0.22 μm organic phase filter membrane. The concentration of tetracycline was measured by high performance liquid chromatography. The column temperature was 30 °C, the flow rate of tetracycline was 1.0 mL/min, the injection volume was 20 μL, the wavelength was 280 nm, and the mobile phase was acetonitrile: 0.01 M oxalic acid = 22: 78. The photocatalytic performance was compared by measuring C/C_0, where C is the concentration of tetracycline at the illumination time t, and C_0 is the initial concentration of tetracycline.

2.Physical Measurements.

Transmission electron microscopy (TEM) measurements were performed on an HT7700 field emission transmission electron microscope with an accelerating voltage of 120 kV. High resolution TEM measurements and energy dispersive X-ray (EDX) measurements were performed on a FEI Talos F200S transmission electron microscope with an accelerating voltage of 200 kV. HAADF-STEM and elemental mapping images were performed on a FEI Talos F200X transmission electron microscope. Powder X-ray diffraction (XRD) results were re-determined by a Rigaku D/MAX-2200 equipped with a rotating anode and a Cu Kα radiation source (λ = 0.15418

nm). Luminescence spectra and lifetime measurements were recorded at room temperature using FS5 (Edinburgh), in conjunction with 980 nm (MDL-III-980) at room temperature. UV-Vis absorption spectra were measured using a PerkinElmer Lambda 750 UV-Vis-NIR spectrometer. All spectra were recorded under the same experimental conditions unless otherwise stated. The key experiment was repeated three times and the other experiments were repeated twice.

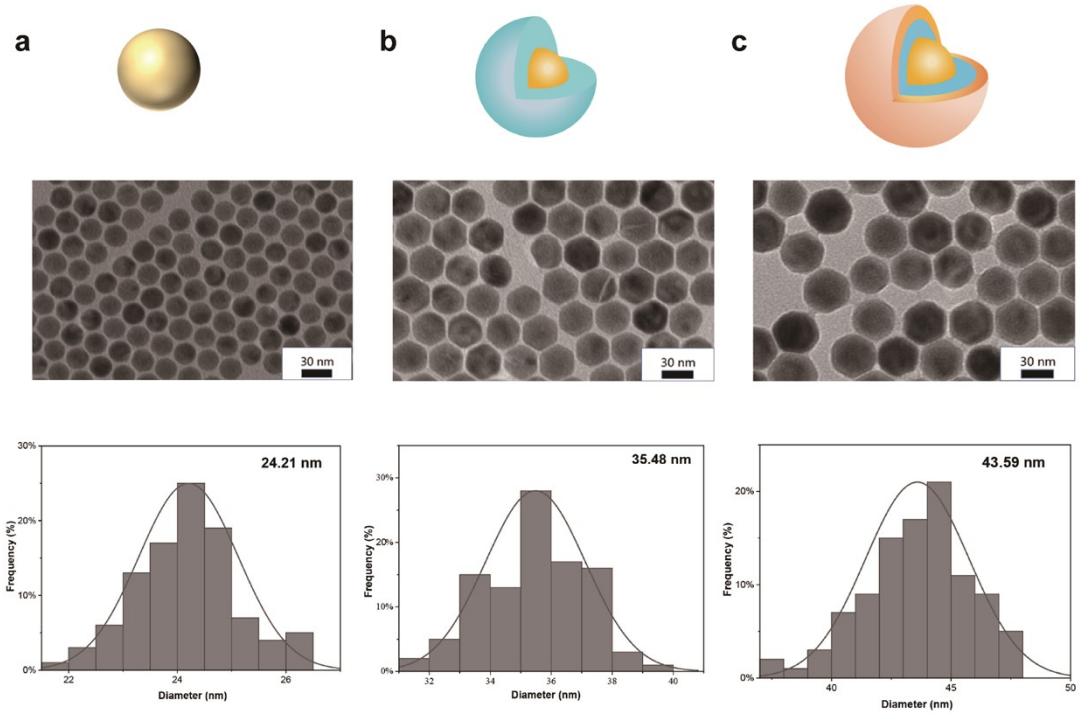

Figure S1. Schematic illustration, TEM images and size distributions of core (a), core-shell (b), core-shell-shell (c), of the as-synthesized $NaYbF_4$@$NaGdF_4$:49%Yb,1%Tm @$NaYF_4$:10%Yb nanocrystal. The size distribution is fitted by a Gaussian curve (black full line).

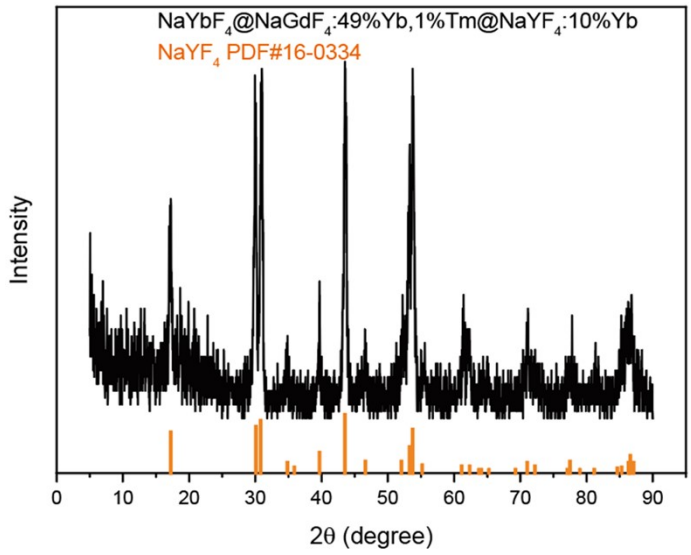

Figure S2. XRD pattern of $NaYbF_4$@$NaGdF_4$:49%Yb,1%Tm@$NaYF_4$:10%Ybnanocrystals.

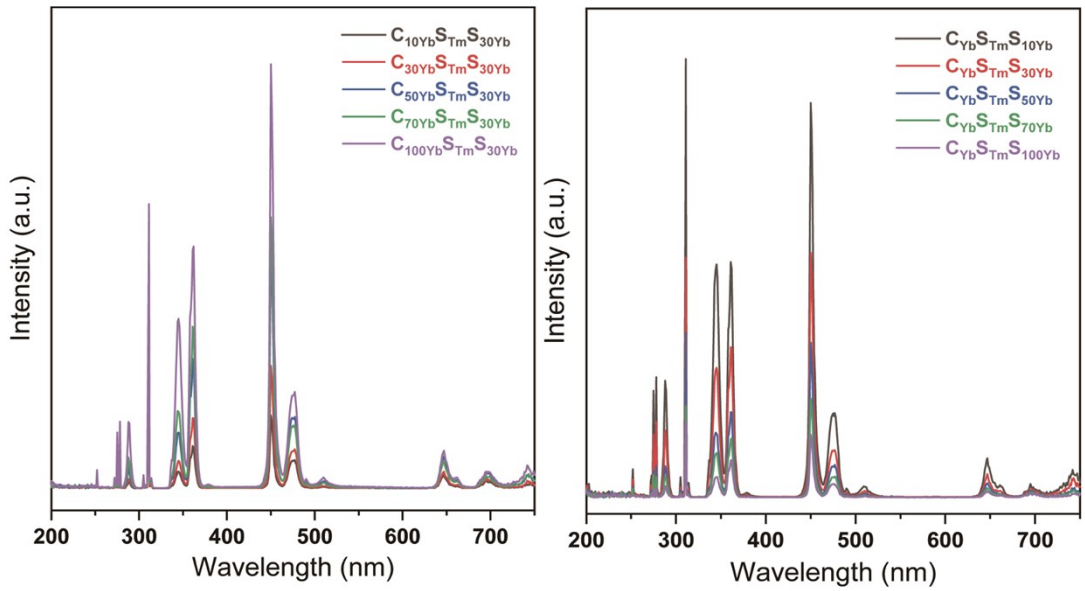

Figure S3. Upconversion emission spectra of $NaYF_4$:X%Yb@$NaGdF_4$:49%Yb,1%Tm@$NaYF_4$:X%Yb core–shell-shell nanocrystals with different amounts of Yb^{3+}.

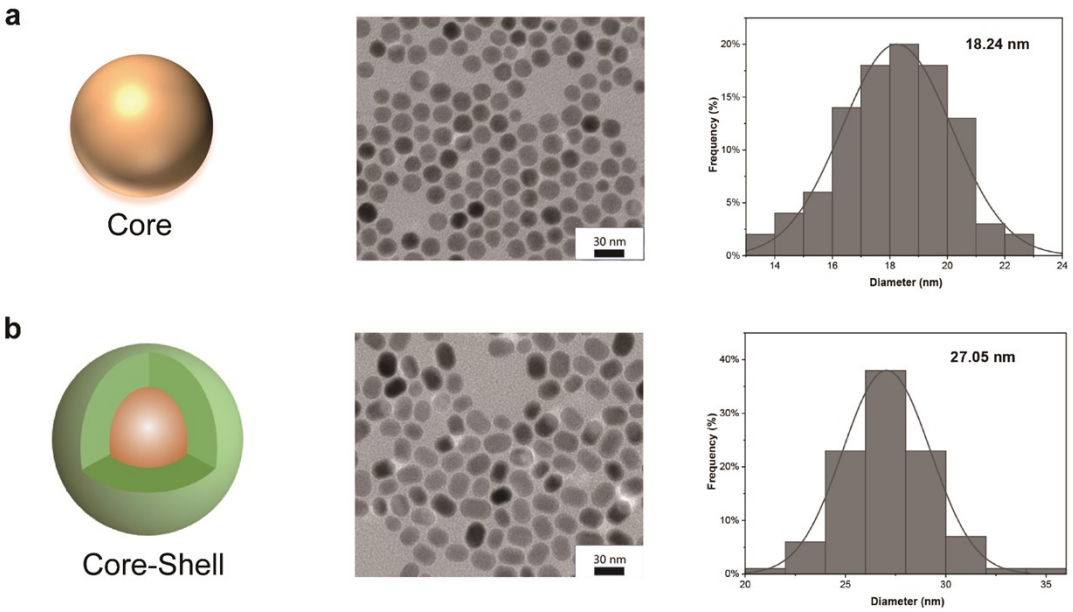

Figure S4. Schematic illustration, TEM images and size distributions of core (a), core-shell (b), of the as-synthesized $NaGdF_4$:49%Yb,1%Tm@$NaYF_4$ nanocrystal. The size distribution is fitted by a Gaussian curve (black full line).

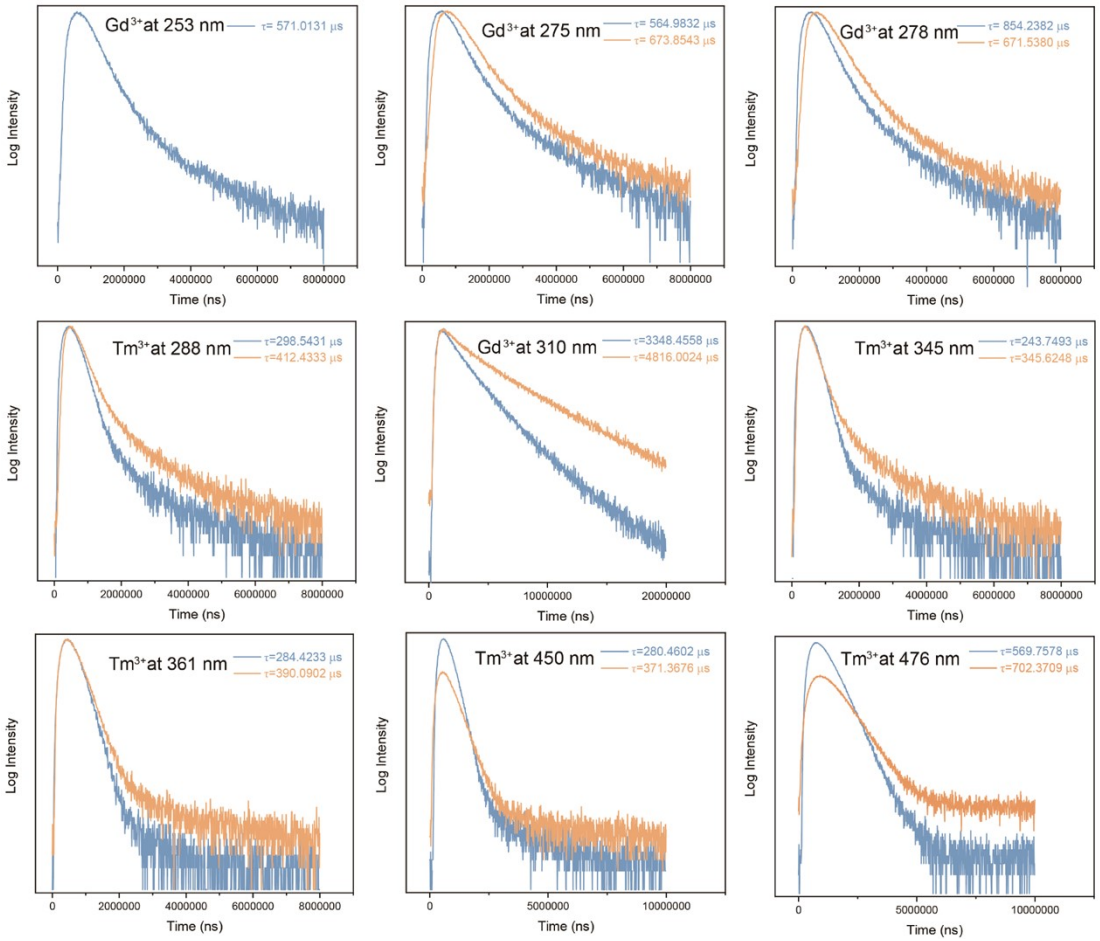

Figure S5. Upconversion luminescence decay curves of Tm^{3+} emissions and Gd^{3+} emissions from $NaYbF_4$@$NaGdF_4$:49%Yb,1%Tm@$NaYF_4$:10%Yb (blue lines)and $NaGdF_4$: 49%Yb,1%Tm@$NaYF_4$ (orange lines)by pulsed 980 nm excitation.

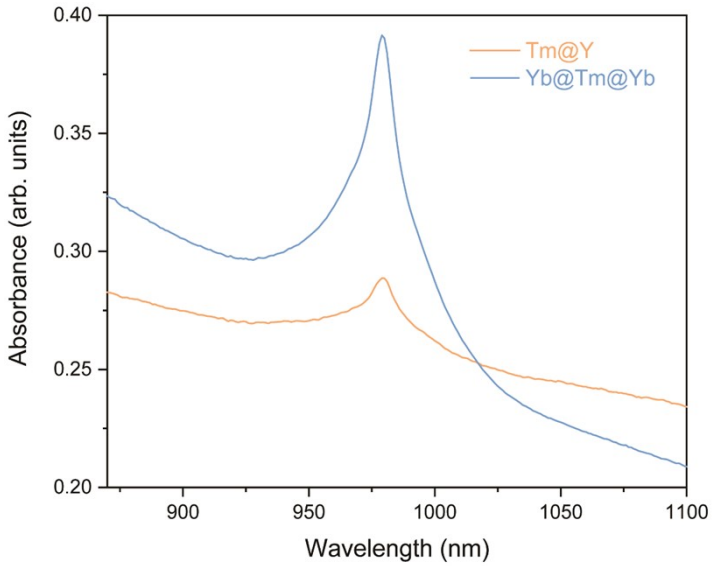

Figure S6. Absorption spectra of Yb@Tm@Yb and Tm@Y nanocystals.

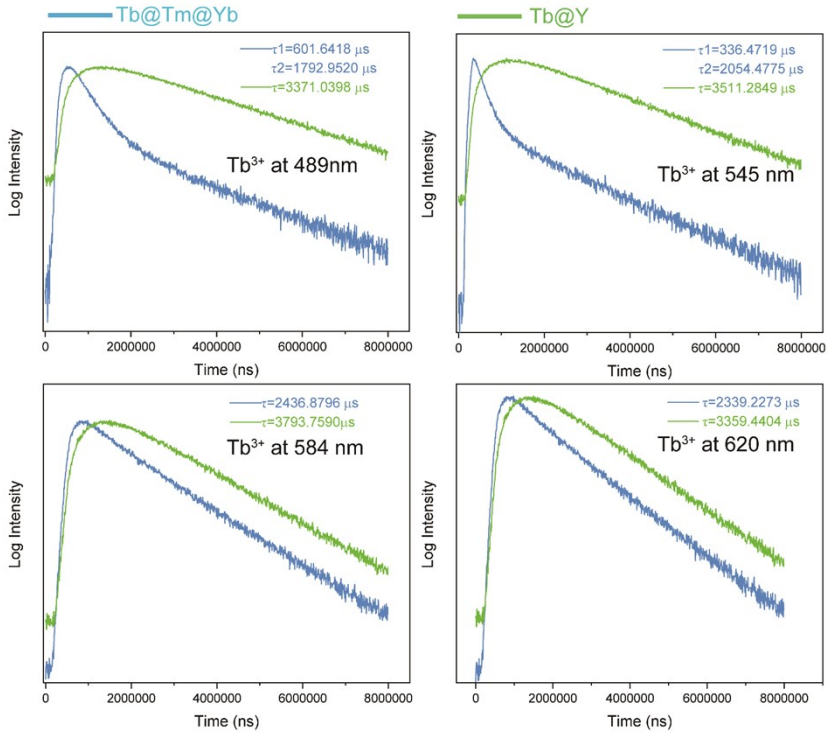

Figure S7. Upconversion luminescence decay curves of Tb^{3+} emissions from $NaYbF_4$:40%Tb@$NaGdF_4$:49%Yb,1%Tm@$NaYF_4$:10%Yb (Tb@Tm@Yb) and $NaYbF_4$:40%Tb@$NaYF_4$ (Tb@Y) by pulsed 980 nm excitation.

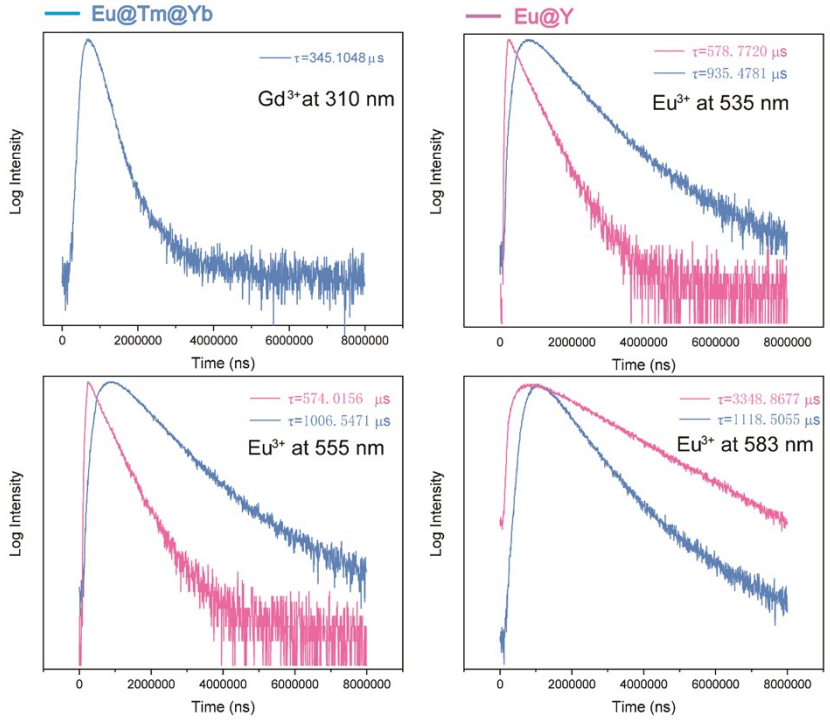

Figure S8. Upconversion luminescence decay curves of Eu^{3+} emissions and Gd^{3+} emissions from $NaYbF_4$:40%Eu@$NaGdF_4$:49%Yb,1%Tm@$NaYF_4$: 10%Yb (Eu@Tm@Yb) and $NaYbF_4$:40%Eu@$NaYF_4$ (Eu@Y) by pulsed 980 nm excitation.

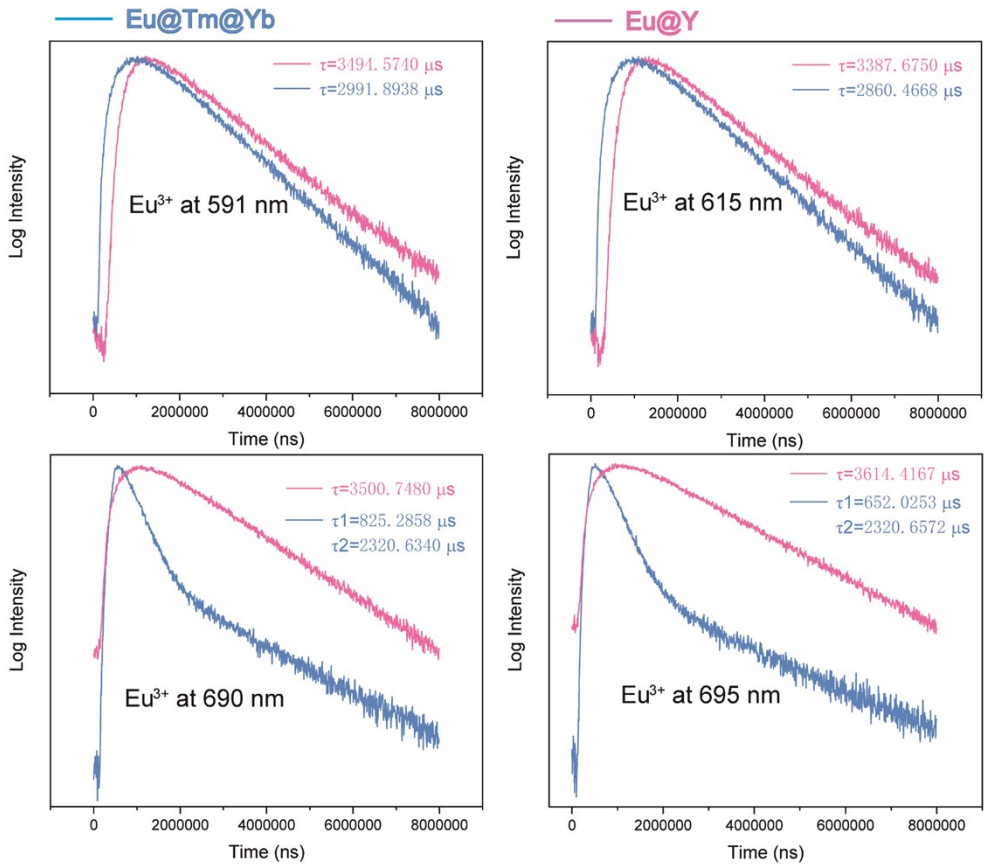

Figure S9. Upconversion luminescence decay curves of Eu^{3+} emissions from $NaYbF_4$:40%Eu@$NaGdF_4$:49%Yb,1%Tm@$NaYF_4$: 10%Yb (Eu@Tm@Yb) and $NaYbF_4$:40%Eu@$NaYF_4$ (Eu@Y) by pulsed 980 nm excitation.

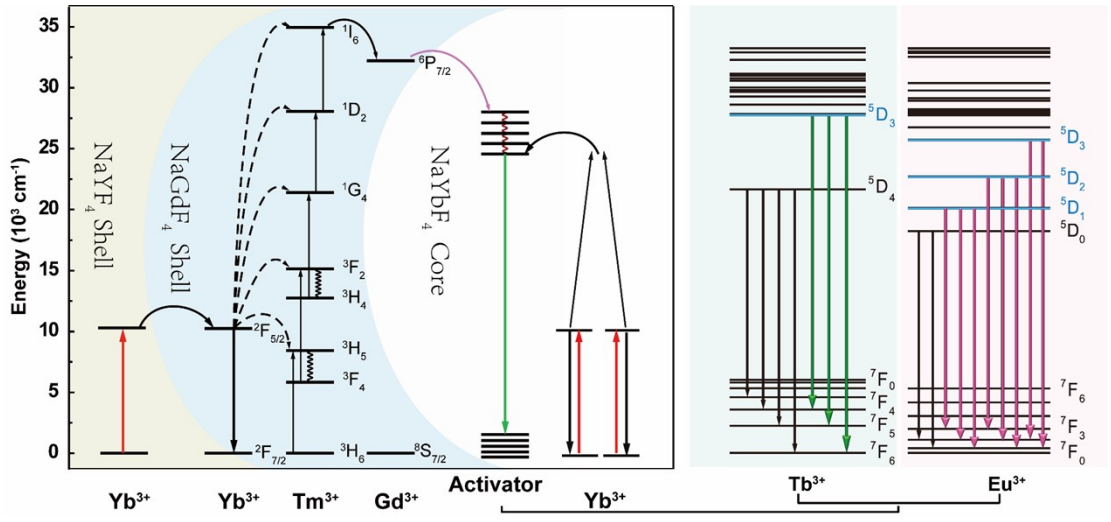

Figure S10. Proposed energy transfer mechanisms in the co-sensitization nanoparticles. Note that only partial energy levels of Tm^{3+}, Gd^{3+}, and A^{3+} (A=Tb and Eu) are shown for clarity. The optical emissions from higher-lying energy levels of Tb^{3+} and Eu^{3+} are highlighted with colored arrows.

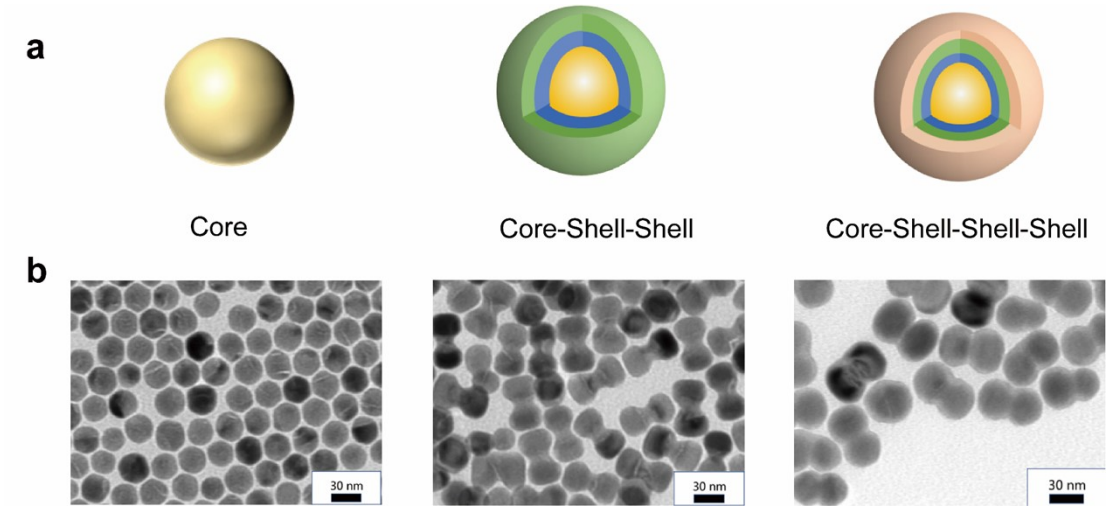

Figure S11. Schematic illustration (a), and TEM images (b) of the as-synthesized $NaYbF_4$@$NaGdF_4$:49%Yb,1%Tm@$NaGdF_4$:10%Yb,5%Dy@$NaYF_4$ (Yb@Tm@5%Dy@Y) nanocrystal.

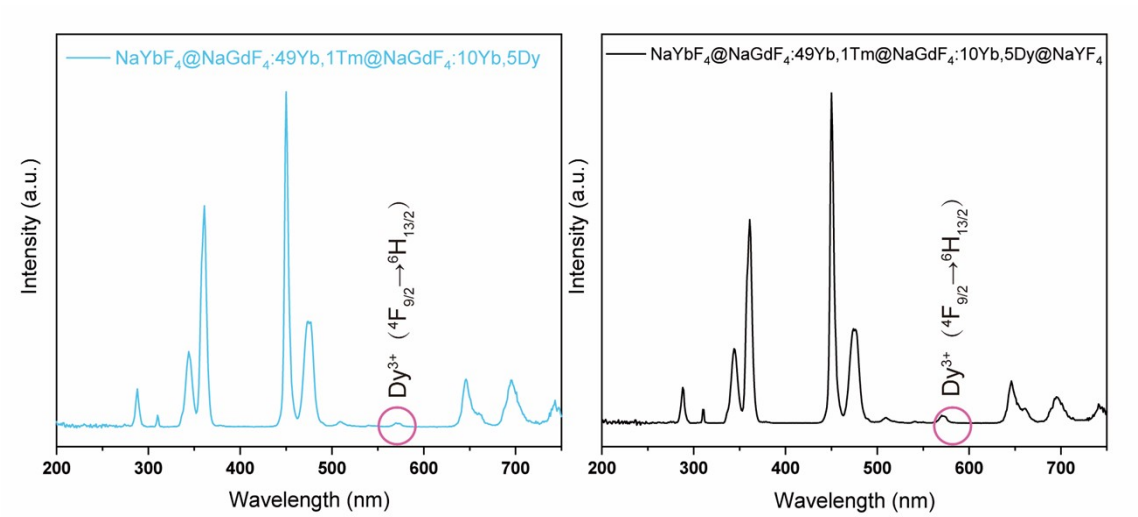

Figure S12. Upconversion emission spectra of $NaYbF_4$@$NaGdF_4$:49%Yb,1%Tm@$NaGdF_4$:10%Yb,5%Dy (Yb@Tm@5%Dy) and $NaYbF_4$@$NaGdF_4$:49%Yb,1%Tm@$NaGdF_4$:10%Yb,5%Dy@$NaYF_4$ (Yb@Tm@5%Dy@Y) nanocrystals under 980 nm excitation.

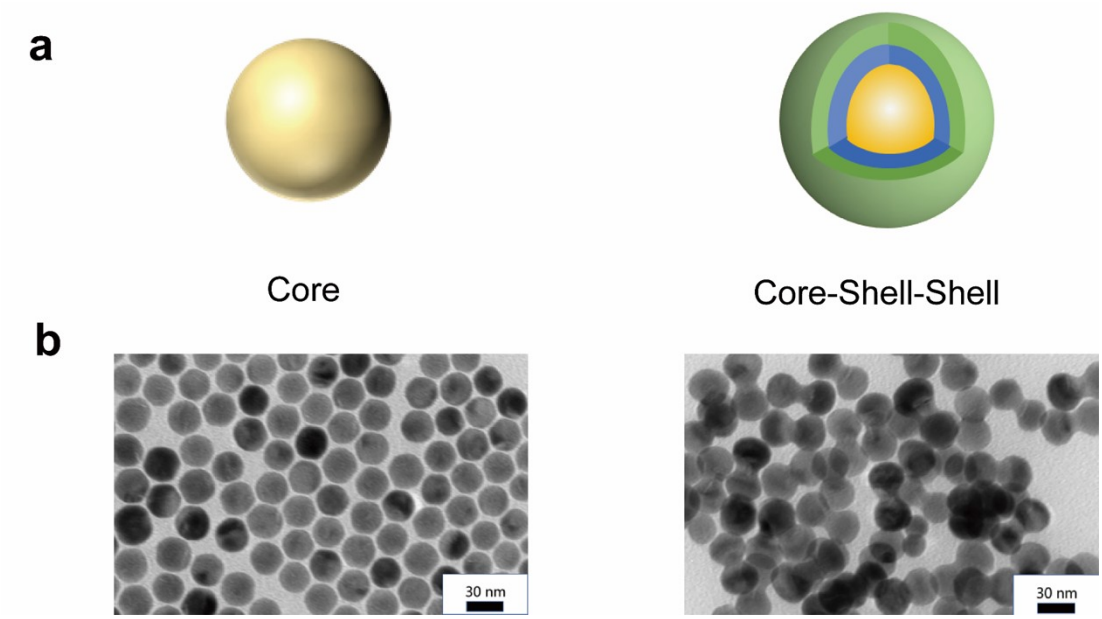

Figure S13. Schematic illustration (a), and TEM images (b) of the as-synthesized $NaYbF_4$@$NaGdF_4$:49%Yb,1%Tm@$NaGdF_4$:10%Yb,1%Dy nanocrystal.

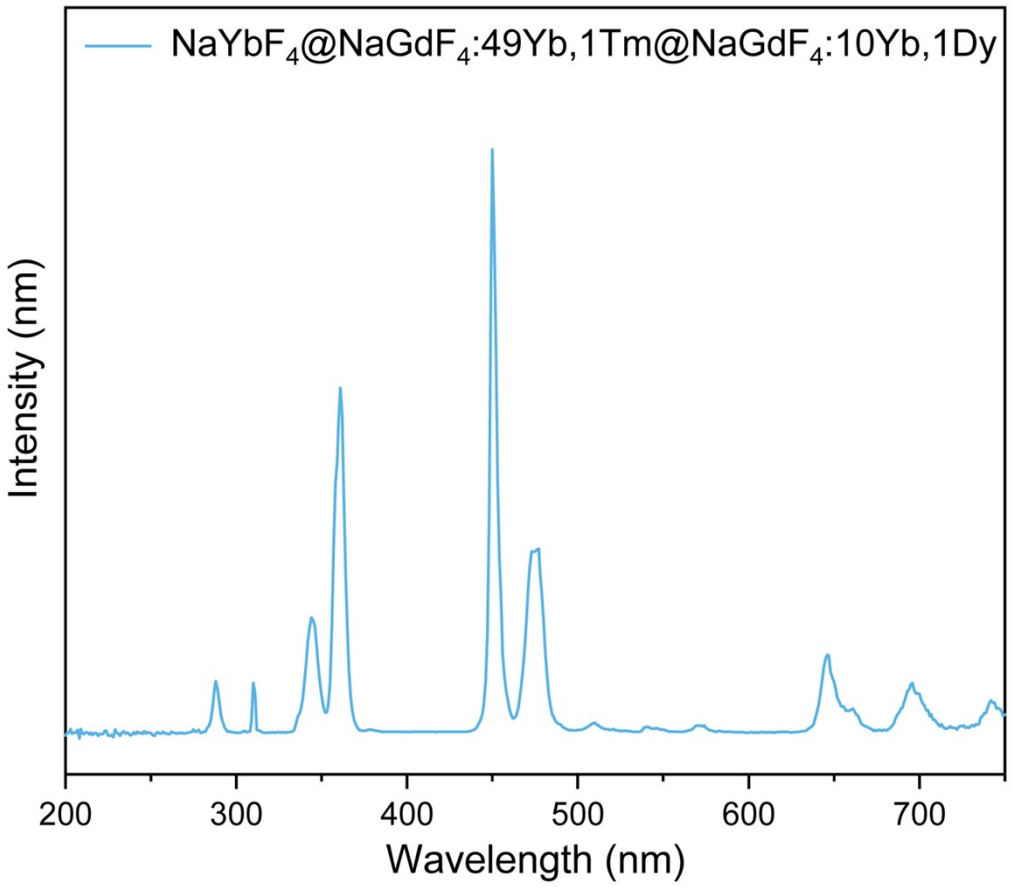

Figure S14. Upconversion emission spectra of $NaYbF_4$@$NaGdF_4$:49%Yb,1%Tm@$NaGdF_4$:10%Yb,1%Dy nanocrystals under 980 nm excitation.

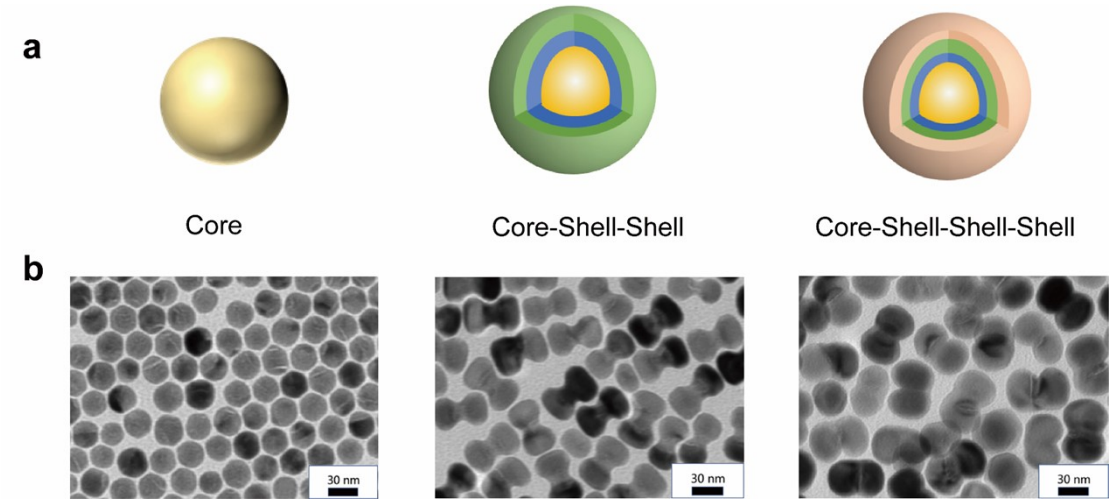

Figure S15. Schematic illustration (a), and TEM images (b) of the as-synthesized $NaYbF_4$@$NaGdF_4$:49%Yb,1%Tm@$NaGdF_4$: 10%Yb,5%Sm@$NaYF_4$ nanocrystal.

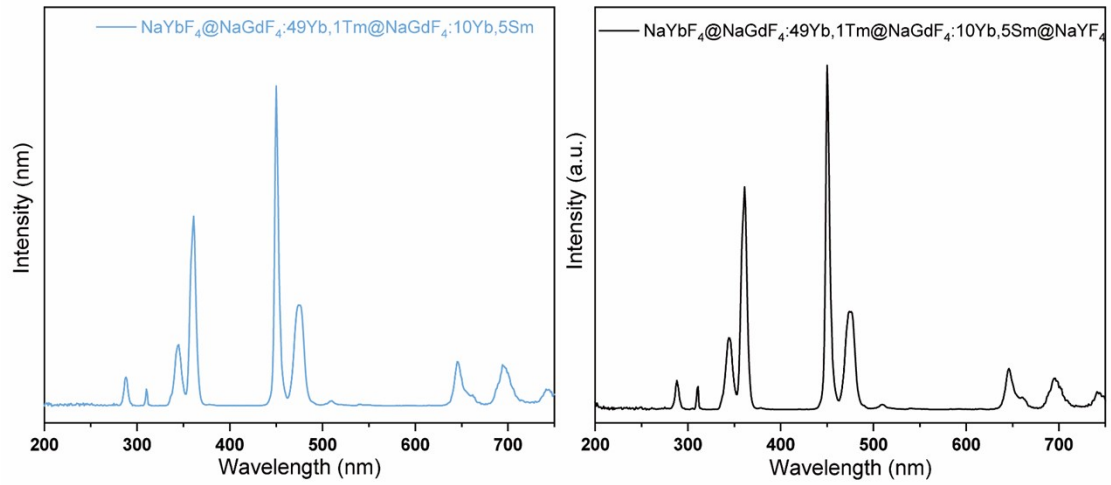

Figure S16. Upconversion emission spectra of $NaYbF_4$@$NaGdF_4$:49%Yb,1%Tm@$NaGdF_4$:10%Yb,5%Sm and $NaYbF_4$@$NaGdF_4$: 49%Yb,1%Tm@$NaGdF_4$:10%Yb,5%Sm@$NaYF_4$ nanocrystals under 980 nm excitation.

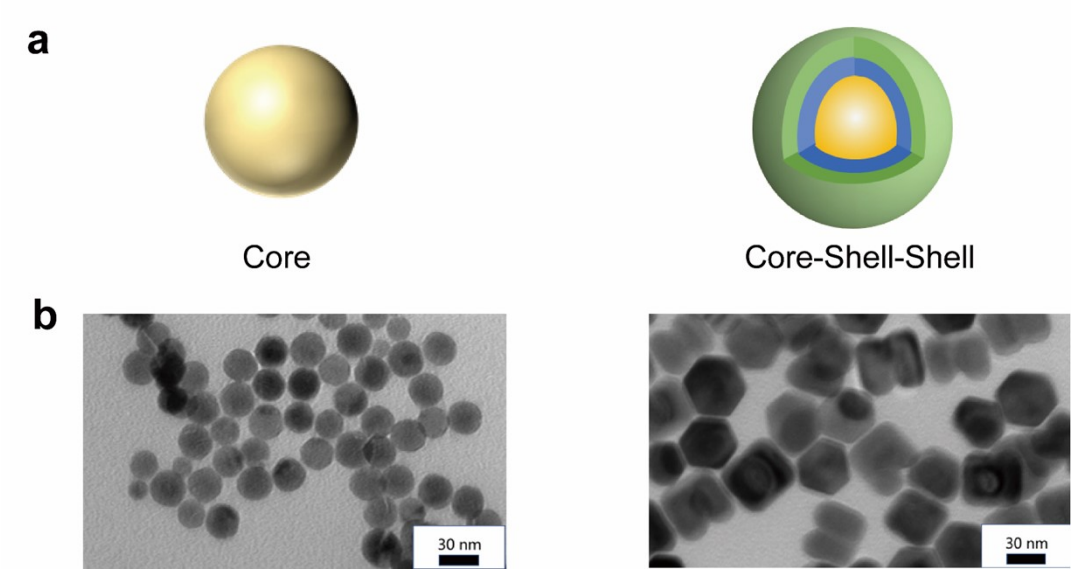

Figure S17. Schematic illustration (a), and TEM images (b) of the as-synthesized $NaYbF_4$@$NaGdF_4$:49%Yb,1%Tm@$NaGdF_4$:10%Yb,1%Sm nanocrystal.

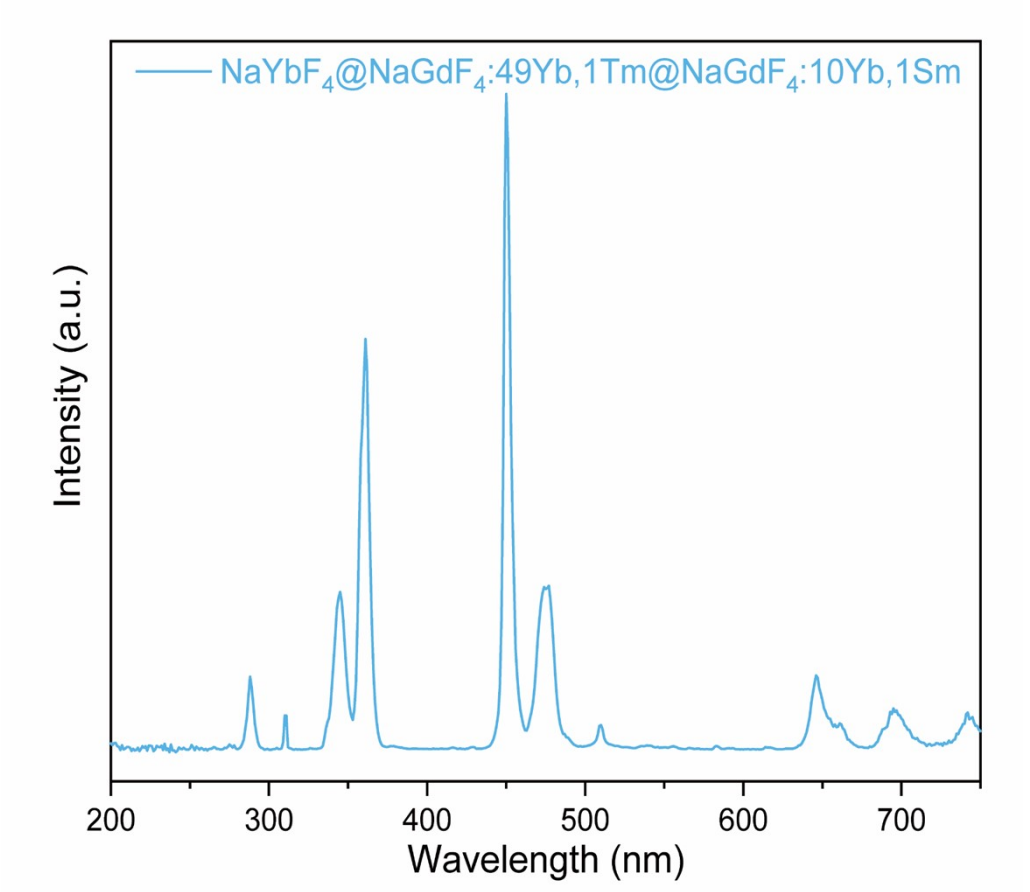

Figure S18. Upconversion emission spectra of $NaYbF_4$@$NaGdF_4$:49%Yb,1%Tm@$NaGdF_4$:10%Yb,1%Sm nanocrystals under 980 nm excitation.

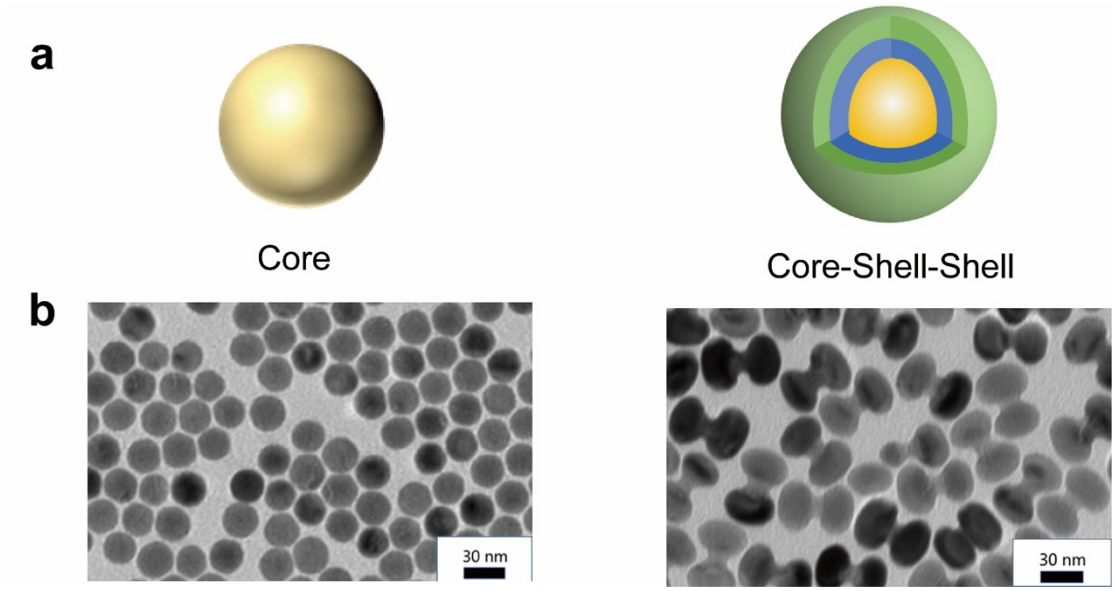

Figure S19. Schematic illustration (a), and TEM images (b) of the as-synthesized $NaYbF_4$@$NaGdF_4$:49%Yb,1%Tm@$NaGdF_4$:10%Yb,15%Ce nanocrystal.

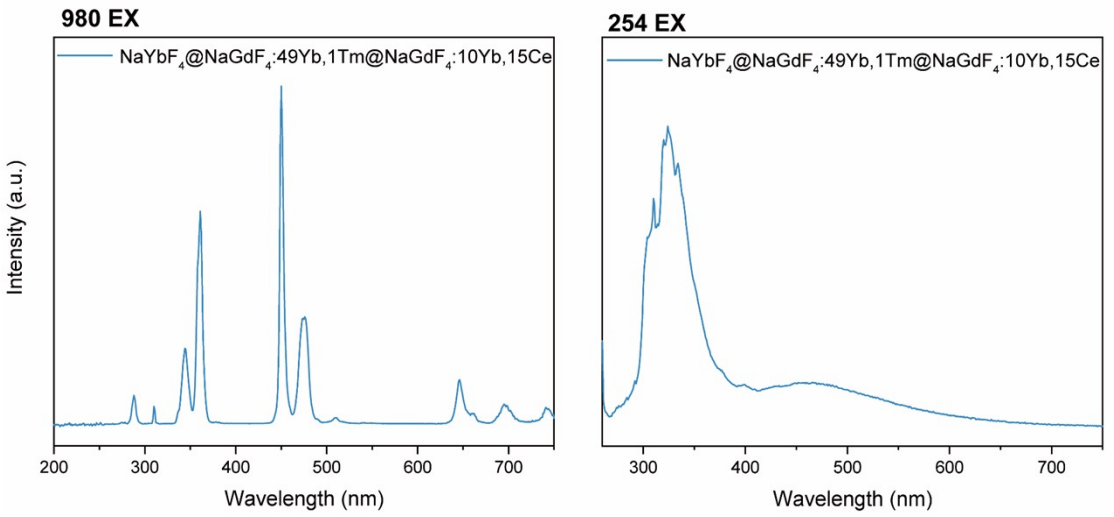

Figure S20. Upconversion and downshifting emission spectra of $NaYbF_4$@$NaGdF_4$:49%Yb,1%Tm@$NaGdF_4$:10%Yb,15%Ce nanocrystals under 980 and 254 nm excitation.

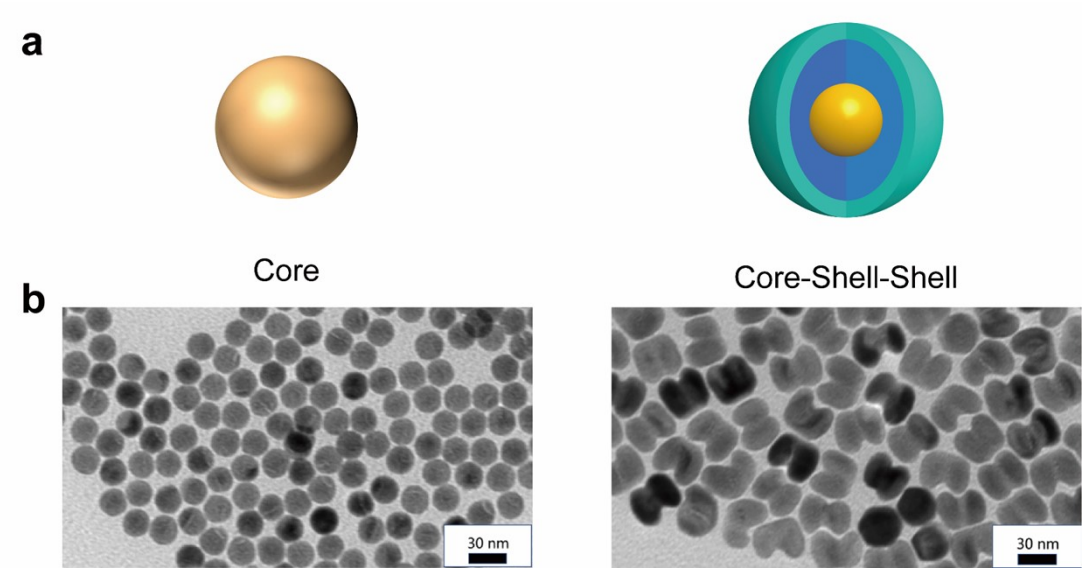

Figure S21. Schematic illustration (a), TEM images (b), of the as-synthesized $NaYbF_4$@$NaGdF_4$:49%Yb,1%Tm@$NaGdF_4$:10%Yb,5%Ce nanocrystal.

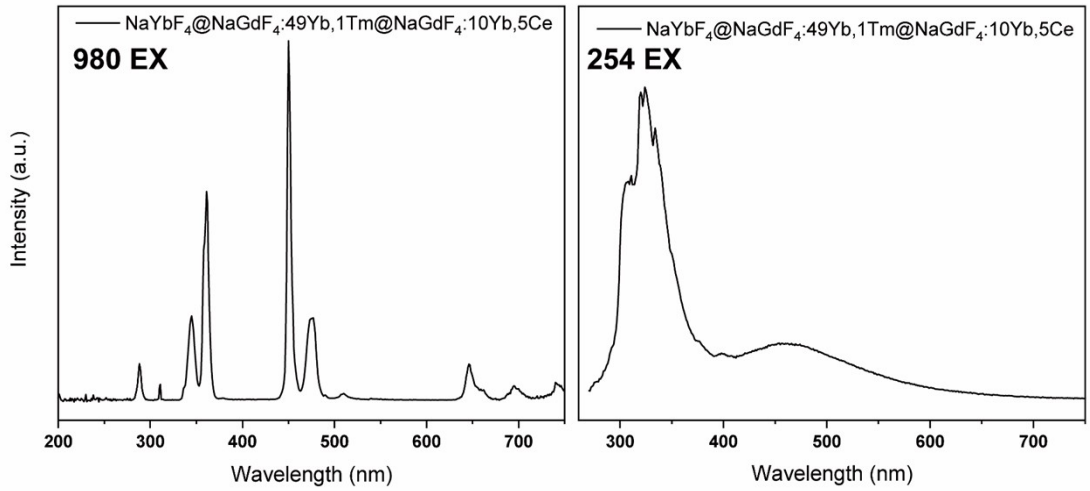

Figure S22. Upconversion and downshifting emission spectra of $NaYbF_4$@$NaGdF_4$: 49%Yb,1%Tm@$NaGdF_4$:10%Yb,5%Ce nanocrystals under 980 and 254 nm excitation.

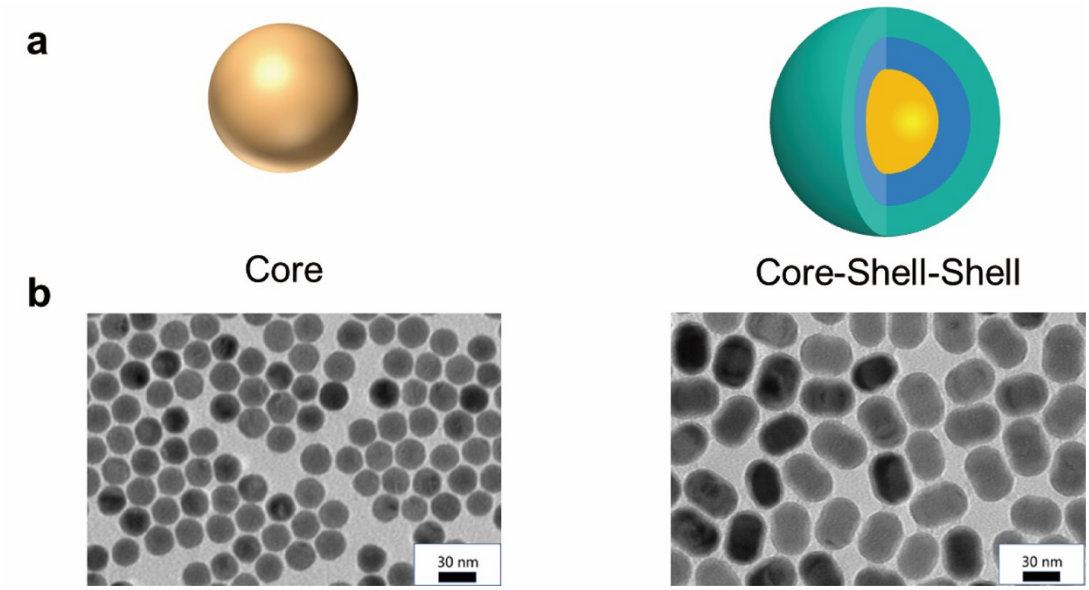

Figure S23. Schematic illustration (a), and TEM images (b) of the as-synthesized $NaYbF_4$@$NaGdF_4$:49%Yb,1%Tm,1%Er@$NaYF_4$: 10%Yb (Yb@Tm,Er@Yb) nanocrystal.

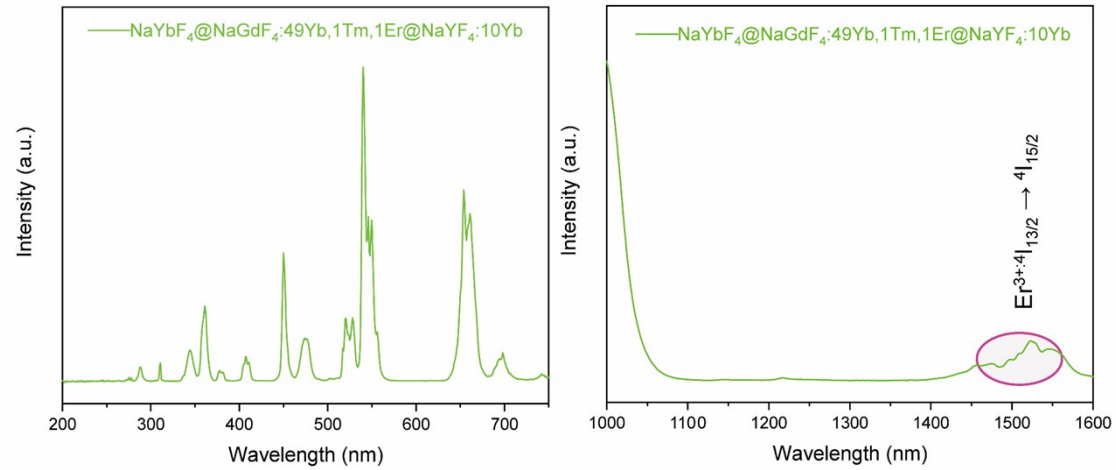

Figure S24. Upconversion and downshifting emission spectra of $NaYbF_4$@$NaGdF_4$:49%Yb, 1%Tm,1%Er@$NaYF_4$:10%Yb (Yb@Tm,Er@Yb) nanocrystals under 980 nm excitation.

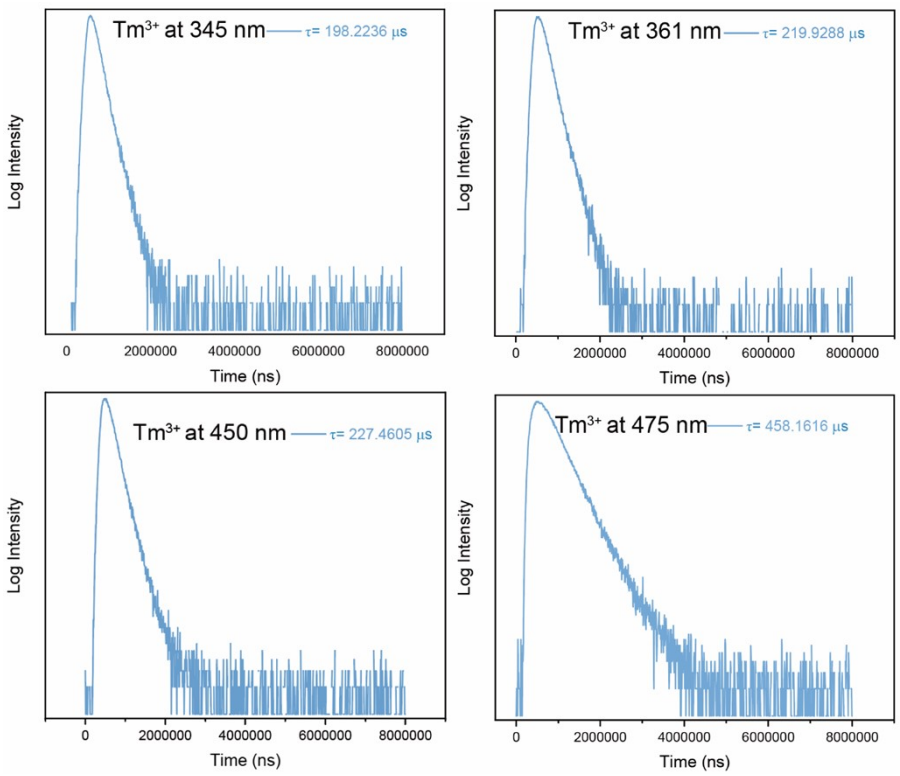

Figure S25. Upconversion luminescence decay curves of Tm^{3+} emissions from Tb@Tm@Yb by pulsed 980 nm excitation.

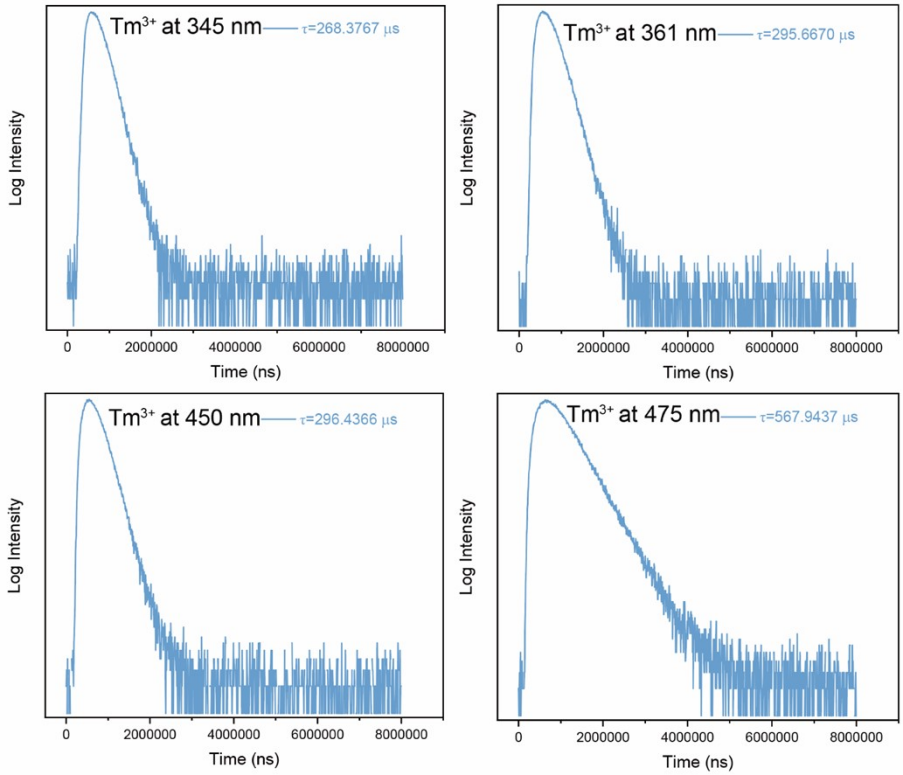

Figure S26. Upconversion luminescence decay curves of Tm^{3+} emissions from Eu@Tm@Yb by pulsed 980 nm excitation.

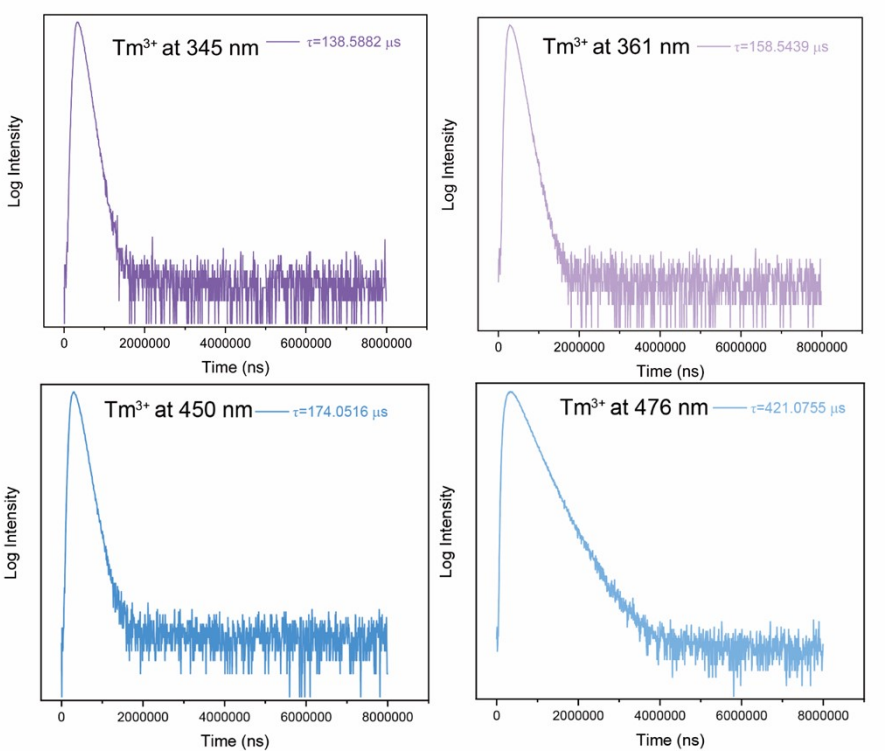

Figure S27. Upconversion luminescence decay curves of Tm^{3+} emissions from Tb@Tm@Eu by pulsed 980 nm excitation.

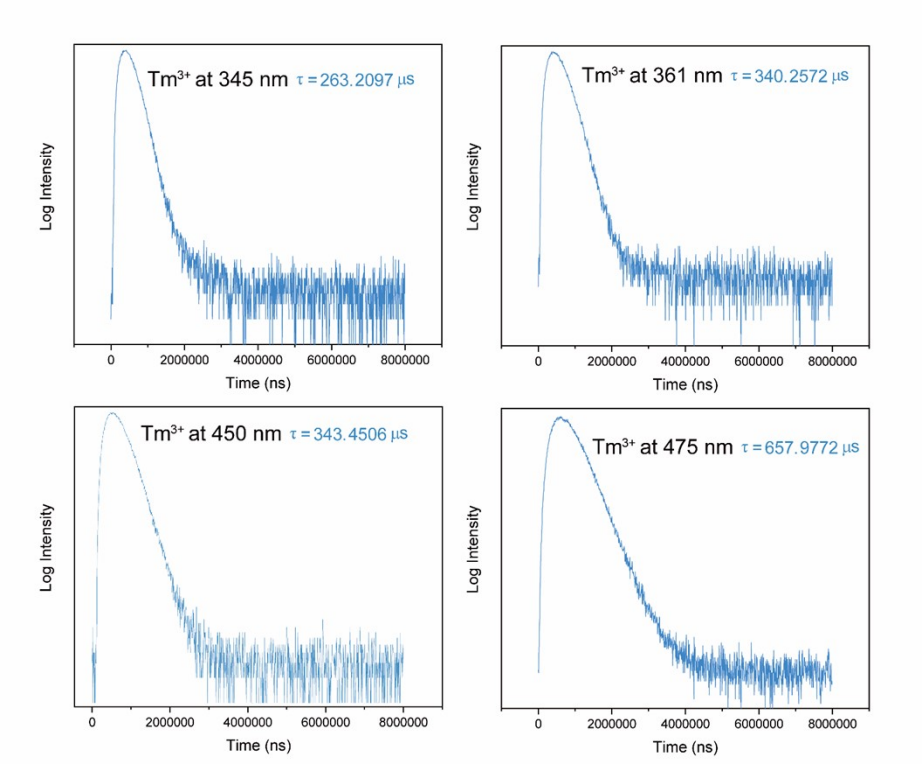

Figure S28. Upconversion luminescence decay curves of Tm^{3+} emissions from Yb@Tm,Er@Yb by pulsed 980 nm excitation.

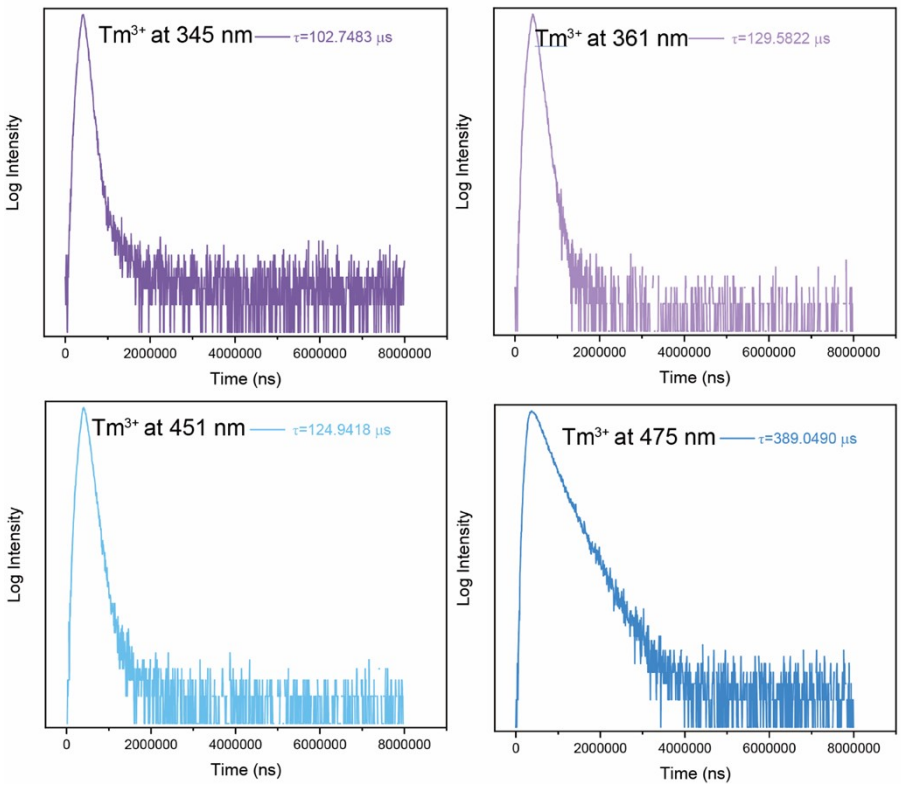

Figure S29. Upconversion luminescence decay curves of Tm^{3+} emissions from Tb@Tm,Er@Eu by pulsed 980 nm excitation.

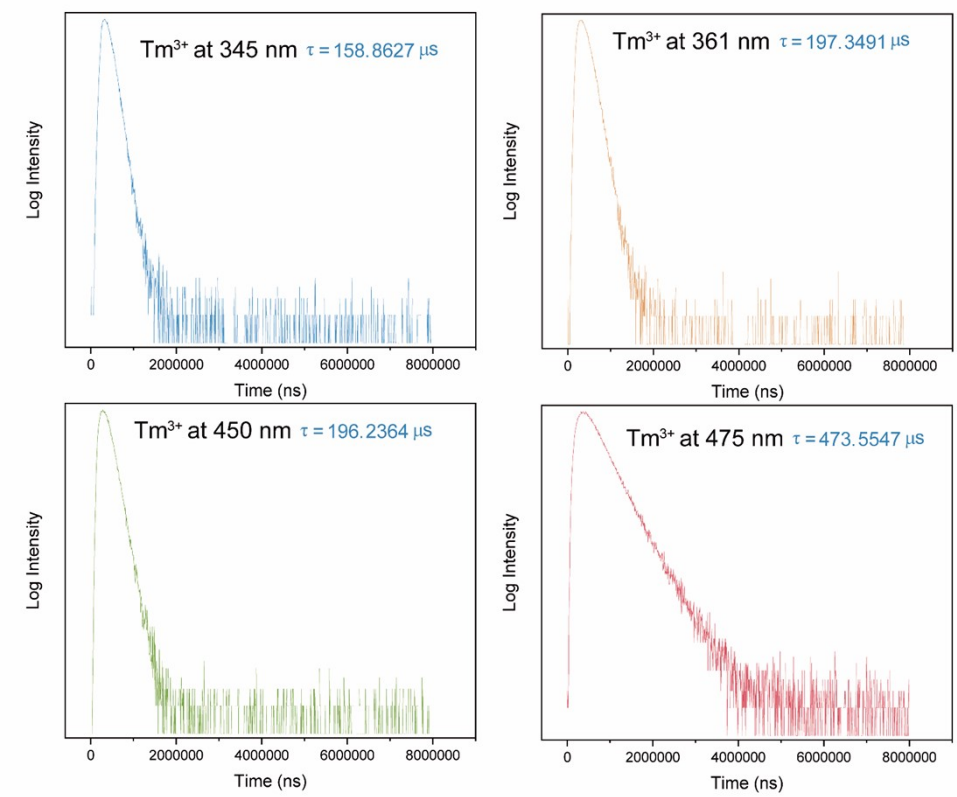

Figure S30. Upconversion luminescence decay curves of Tm^{3+} emissions from Yb@Tm@15%Ce by pulsed 980 nm excitation.

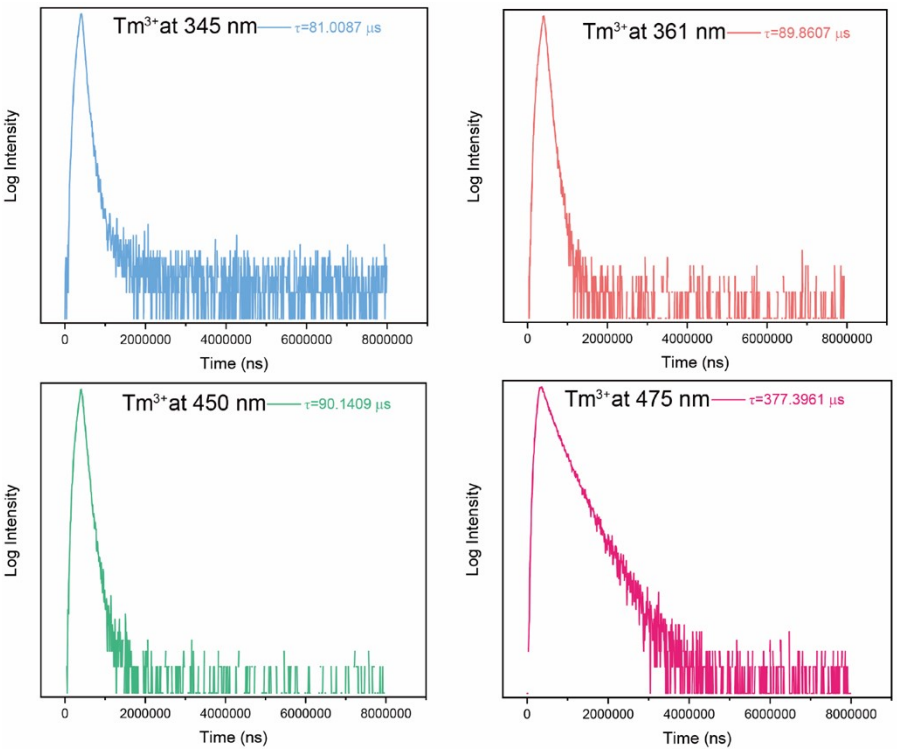

Figure S31. Upconversion luminescence decay curves of Tm^{3+} emissions from Yb@Tm@5%Dy by pulsed 980 nm excitation.

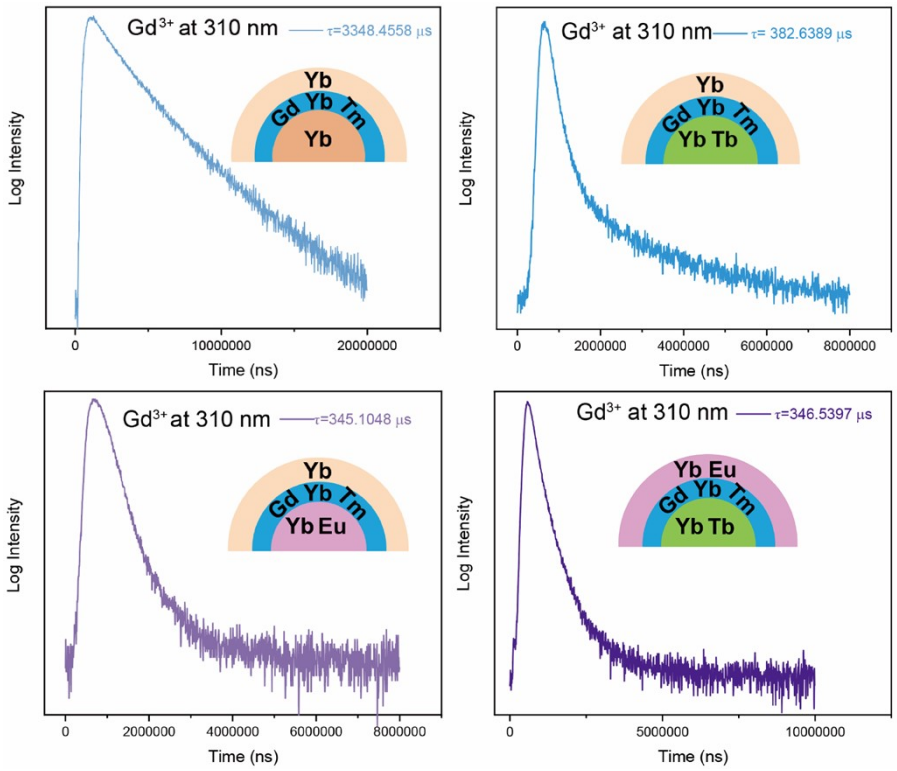

Figure S32. Upconversion luminescence decay curves at 310 nm for Gd^{3+} ions in Yb@Tm@Yb,Tb@Tm@Yb,Eu@Tm@Yb and Tb@Tm@Eu by pulsed 980 nm excitation.

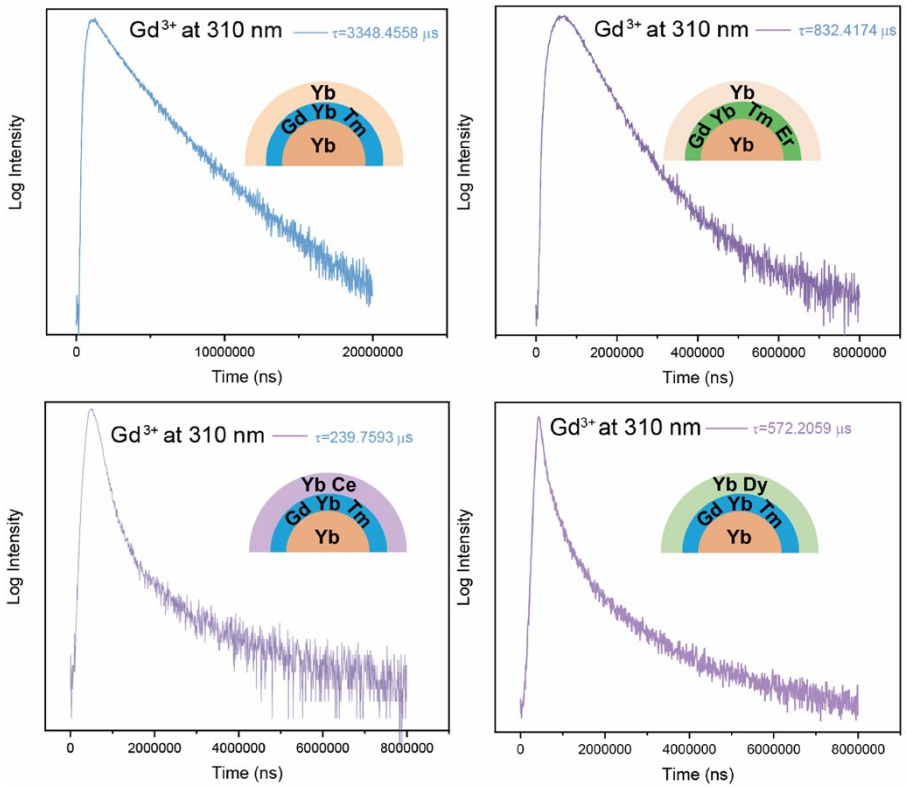

Figure S33. Upconversion luminescence decay curves at 310 nm for Gd^{3+} ions in Yb@Tm@Yb, Yb@Tm,Er@Yb, Yb@Tm@15%Ce and Yb@Tm@5%Dy by pulsed 980 nm excitation.

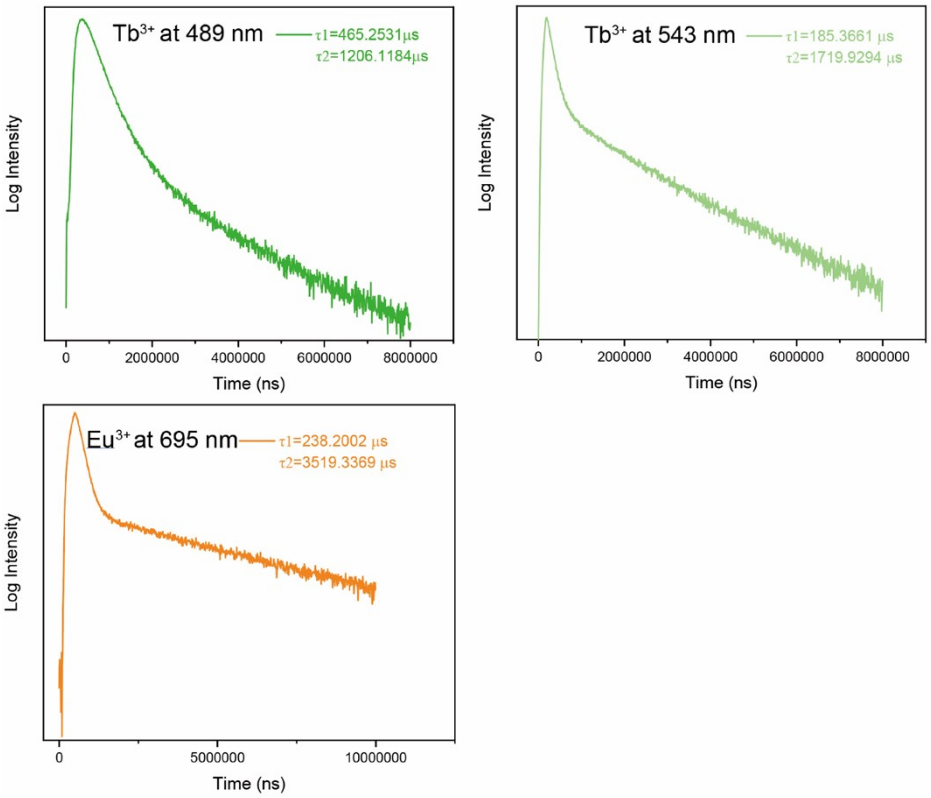

Figure S34. Upconversion luminescence decay curves from Tb^{3+} and Eu^{3+} ions in Tb@Tm@Eu by pulsed 980 nm excitation.

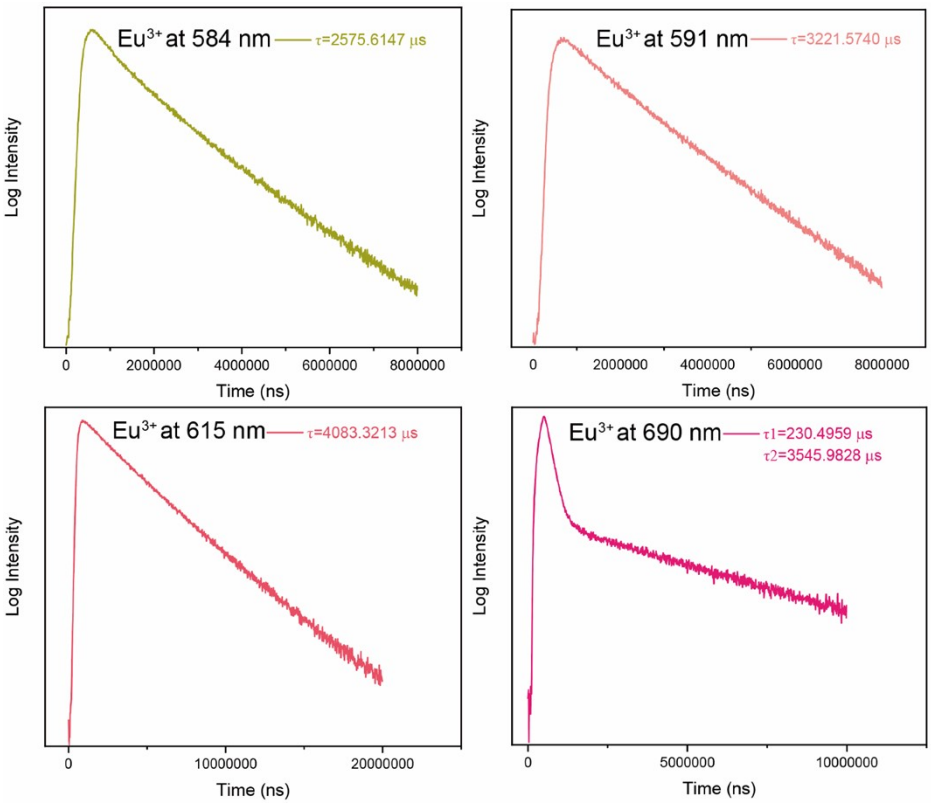

Figure S35. Upconversion luminescence decay curves from Eu^{3+} ions in Tb@Tm@Eu by pulsed 980 nm excitation.

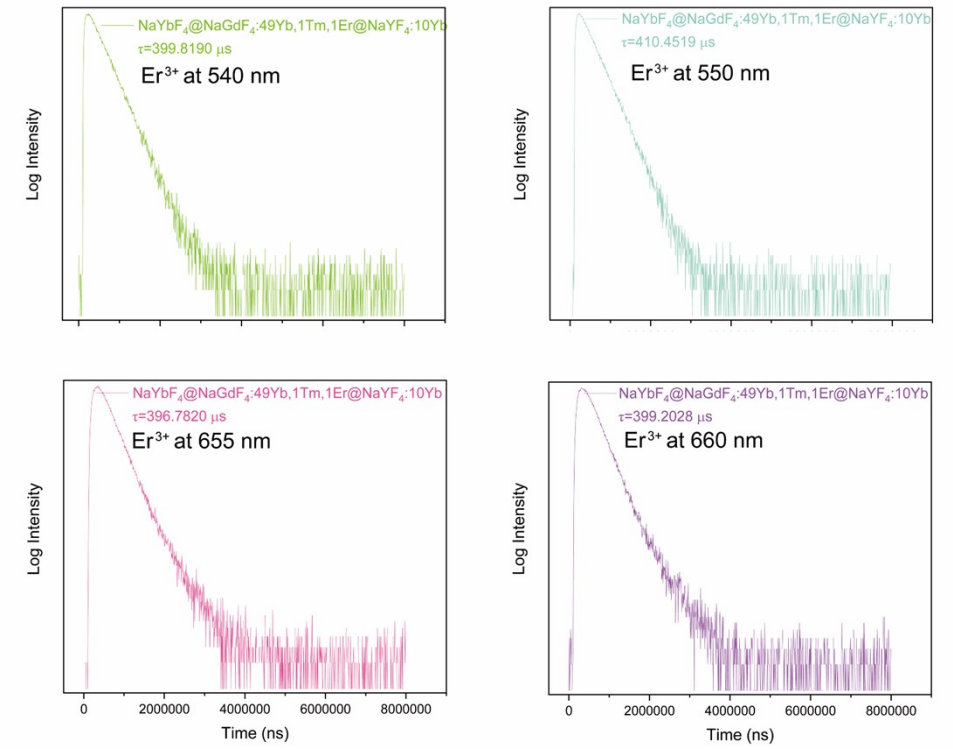

Figure S36. Upconversion luminescence decay curves from Er^{3+} ions in Yb@Tm,Er@Yb by pulsed 980 nm excitation.

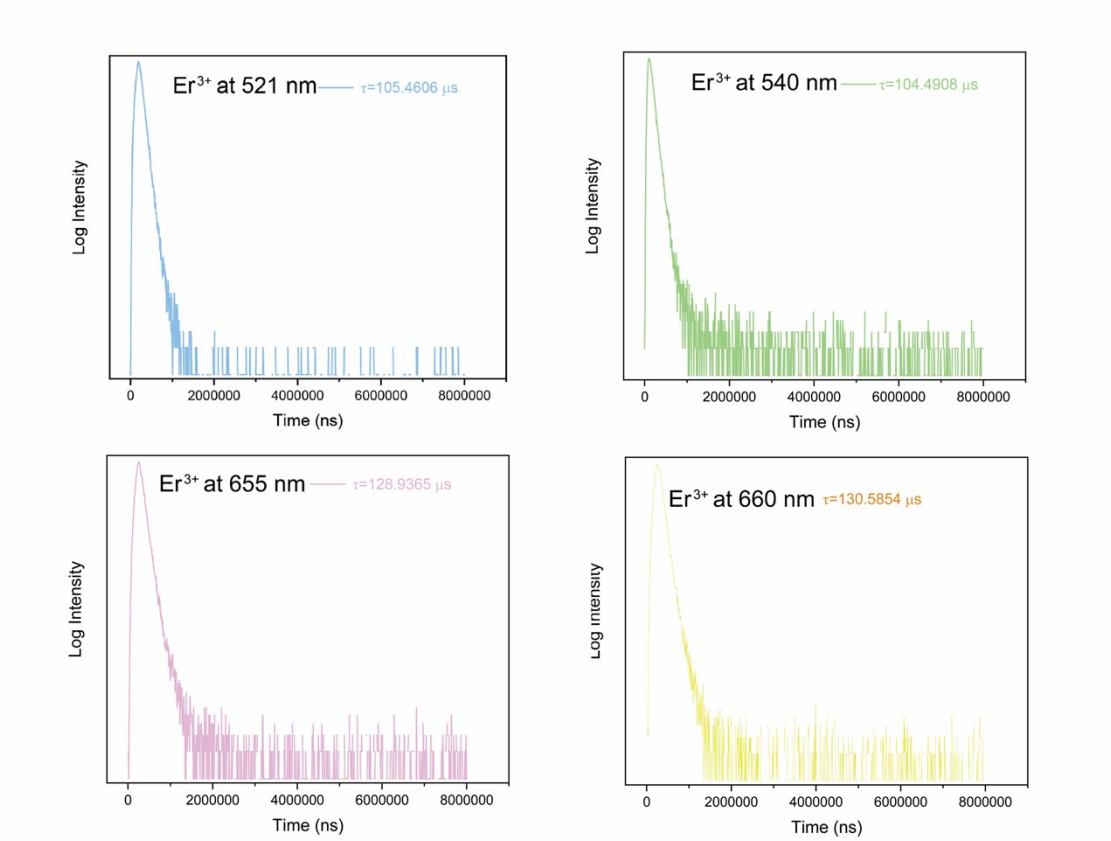

Figure S37. Upconversion luminescence decay curves from Er^{3+} ions in Tb@Tm,Er@Eu by pulsed 980 nm excitation.

References

[1] R. Shi, X. Ling, X. Li, L. Zhang, M. Lu, X. Xie, L. Huang and W. Huang. *Nanoscale*, 2017, **9**, 13739-13746.

[2] Q. Q. Su, H. L. Wei, Y. C. Liu, Chen, M. Guan, S. Wang, Y. Su, H. Wang, Z. Chen and D. Y. Jin, *Nat. Commun*, 2021, **12**, 4367.

[3] H. N. Huang, H. L. Li, Z. Y. Wang, P. Wang, Z. K. Zheng, Y. Y. Liu, Y. Dai, Y. J. Li and B. B. Huang, *Chem. Eng. J*., 2019, **361**, 1089-1097.

[4] Z. Y. Hou, Y. X. Zhang, K. R. Deng, Y. Y. Chen, X. J. Li, X. R. Deng, Z. Y. Cheng, H. Z. Lian, C. X. Li and J. Lin, *ACS Nano*, 2015, **9**, 2584-2599.

[5] A. Kumar, K. L. Reddy, S. Kumar, A. Kumar, V. Sharma and V. Krishnan, *ACS Appl. Mater. Inter*., 2018, **10**, 15565-15581.